GLOBAL URBAN AREA MAPPING IN HIGH RESOLUTION USING ASTER SATELLITE IMAGES

Hiroyuki Miyazaki [a], Xiaowei Shao [a], Koki Iwao [b], Ryosuke Shibasaki [a]

[a] Center for Spatial Information Science, The University of Tokyo, 435 General research bldg., 5-1-5 Kashiwanoha, Kashiwa, Chiba 277-8568, Japan – heromiya@csis.u-tokyo.ac.jp, shaoxw@iis.u-tokyo.ac.jp, shiba@csis.u-tokyo.ac.jp
[b] National Institute of Advanced Industrial Science and Technology, Tsukuba Central 2, Umezono 1-1-1, Tsukuba, Ibaraki 305-8568, Japan – iwao.koki@aist.go.jp

KEY WORDS: urban area mapping, ASTER, land cover classification

ABSTRACT:

We present development of automated algorithm for mapping global urban area in high resolution using ASTER satellite images and coarse-resolution urban area maps. The algorithm consists of two steps: classifying pixels of ASTER satellite images into urban or non-urban by Learning with Global and Local Consistency (LLGC) technique; and integration with existing urban area maps using logistic regression. We implemented the algorithm and demonstrated it against 340 scenes of ASTER satellite images. LLGC trimmed up 500-m-resolution clusters of urban area into 15-m-resoluton clusters. However accuracy assessment on LLGC result showed 75% user's accuracy, 41% producer's accuracy, 94% overall accuracy and 0.50 kappa coefficient, indicating LLGC had considerable misclassifications due to similarity in surface reflectance among non-vegetative land cover. To complement the misclassifications, we integrated LLGC result with existing urban area maps. Accuracy assessment on result of the integration showed 74% user's accuracy, 43% producer's accuracy, 94% overall accuracy and 0.51 kappa coefficient, indicating that the results were more accurate than LLGC result and existing urban area maps. We concluded our method would improve global urban area map not only in terms of spatial resolution, but also in that of accuracy.

1. INTRODUCTION

Urbanization has been a main concern for regional and global environmental change (Foley et al., 2005) and socio-economic problems (Angel et al., 2005). Various kinds of studies (e.g. Balk et al., 2005; Scholes and Biggs, 2005; Montgomery, 2008; Sutton et al., 2009), have used satellite-derived global urban area maps to evaluate critical aspects of urbanization for global environmental change, such as size, scale and form of cities and conversion of land cover (Laumann, 2005). The studies using global urban area map had provided valuable information of urbanization especially for less documented regions. As the studies on urbanization progressed, however, 1-km spatial resolution of global urban area map have gotten obsolete for measuring spatial structure of urban area in fine scale (Angel et al., 2005) and for modelling land use conversion with socio-economical variables (Nelson and Robertson, 2007).

To measure spatial structure of urban area in fine scale, urban areas in region of interest have to be mapped using high-resolution satellite images (e.g. Landsat, Terra/ASTER, IKONOS and Quickbird). However, classification of urban area from high-resolution satellite images is much time- and labour-consuming, which prevents not only effective investigation in urbanization but also comprehensive comparison over regions and countries. Thus we believe that developing and providing high-resolution global urban area map would promote deeper understanding of urbanization.

In this paper, we present automatic algorithm for developing global urban area map from high-resolution satellite images using Learning with Local and Global Consistency (LLGC) technique and integration with existing urban area maps using logistic regression. Regarding definition of urban, we introduced definition discussed by Potere and Schneider (2007) ; they defined urban with presence of built-up area.

2. METHOD

We constructed the method with two steps: first, we classified urban area from high-resolution satellite images using Learning with Local and Global consistency (LLGC) technique; second, to correct misclassification of LLGC, we integrated the urban area map of LLGC with existing urban area map of coarse resolution. The procedure in each step is described below; overview of the method is showed in Figure 1.

2.1 Classifying Urban Area from ASTER/VNIR Satellite Images using LLGC

To achieve automatic classification of urban area from satellite images, two basic components of classification, clustering and labelling, have to be automated. For automated clustering, unsupervised clustering method (e.g. ISODATA) is commonly employed for land cover classification (e.g. Koeln et al., 2000; Angel et al., 2005); for labelling, however, visually interpreting clusters into land cover classes is needed because clusters does not have any information of land cover class.

For automated labelling, we employed urban area map of coarse resolution as training data. Successfully classified urban area map would be a good training data for clustered satellite images; however the gap of spatial resolution makes inconsistency among pixel values and labels. For example, if a cluster likely to be urban and another cluster likely to be non-urban are covered within an urban pixel of coarse resolution, each cluster includes training data of urban even though they should be separated into urban and non-urban.

To deal with the gap of spatial resolution, we introduced Learning with Local and Global Consistency (LLGC). LLGC constructs a function to correct roughly labelled classification into smoothly labelled result (Zhou et al., 2003). The method was thus suitable for our case, in which clusters derived from

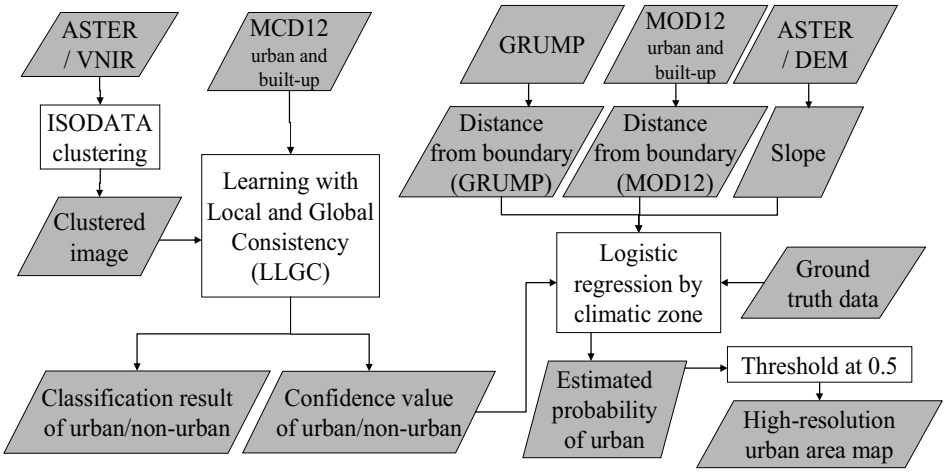

Figure 1. Overview for mapping urban area in high resolution

high-resolution satellite images were initially labelled with coarse-resolution urban area map.

The output of LLGC has not only classification result, but also confidence value ranged from 0 to 1. The confidence value was rather appropriate to represent gradual transition of land cover between urban and rural area. In order to reflect the transition to output, we introduced the confidence value into integration mentioned below.

We employed surface reflectance images derived from Visible and Near-Infrared Radiometer of Advanced Spaceborne Thermal Emission and Reflection radiometer (ASTER/VNIR), which have been commonly used for monitoring urban environment. 15-m spatial resolution of ASTER/VNIR is much finer than existing global urban area map, thus urban area map derived from ASTER/VNIR would allow measuring complex spatial structure of urban area. Moreover, ASTER/VNIR has been operated since December in 1999 to complete cloud-free global coverage (Yamaguchi et al., 1998); therefore we supposed that ASTER/VNIR was the most suitable source for high-resolution global urban area map.

2.2 Integrating with Existing Urban Area Map using Logistic Regression

Although the clusters were successfully classified by LLGC, the result would include misclassifications due to similarity in surface reflectance among different land covers. For example, urban area surrounded with sand area could be classified as non-urban because surface reflectance of urban is similar to sand area. Also, cloud cover would considerably lead to misclassification. These disturbances stem from heterogeneities of landscape and image quality among ASTER/VNIR scenes, suggesting the results would have uncertainty by scene.

To reduce the uncertainties among scenes, we integrated the result of LLGC with existing urban area maps by introducing logistic regression. Logistic regression has an advantage in representing presence of urban in form of probability, which could represent spatial gradual transition between urban and rural area.

We also considered geographical heterogeneity in accuracy of existing urban area maps. Schneider et al. (2003) had suggested that accuracy of satellite-based estimation of urban area at urban centre is higher than at rural area. We expected that distance from boundary of urban area (DBU) would work as proxy of the heterogeneity. We calculated DBU from urban class cluster of MODIS/Terra Land Cover Type 96-Day L3 Global 1km ISIN Grid V004 (MOD12) and GRUMP Urban Extent Grid (GRUMP).

Terrain is also significant factor for presence of urban (Clarke et al., 1997). Therefore we included slope calculated from digital terrain model (DEM) derived from ASTER/VNIR into the logistic regression.

We constructed a model to estimate probability of presence of urban as equation (1).

$$P(urban) = \frac{\exp(U_i)}{1+\exp(U_i)} \quad (1)$$

where $P_i(urban)$ is the probability of presence of urban at ith pixel and U_i is defined in form of polynomial expression as equation (2).

$$U_i = \beta_0 + \beta_1 \times LLGC_i + \beta_2 \times SLOPE_i + \beta_3 \times DIST_{MOD12,i} + \beta_4 \times DIST_{GRUMP,i} \quad (2)$$

where β is coefficient for each variable, $LLGC_i$ is confidence value of $LLGC$ at ith pixel, $SLOPE_i$ is slope at ith pixel, $DBU_{MOD12,i}$ and $DBU_{GRUMP,i}$ is DBU at ith pixel in MOD12, GRUMP, respectively (positive value for outside urban area; negative value for inside urban area).

3. EXPERIMENT AND RESULT

3.1 Sampling ASTER/VNIR Scenes and Ground Truth Data

For experiment, we sampled ASTER/VNIR images by following group:

Group A: randomly selected scenes under stratification in terms of number of cities by climatic zone (7 scenes for tropical; 13 for dry; 55 for temperate; 24 for cold).
Group B: scenes intersecting with urban area of cities of more than one million (241 scenes).

On each scene of Group A, approximately 500 point coordinates were sampled at lattice grid; whereas, on the scenes of Group B, 799 point coordinates were sampled from GRUMP/Settlement Point database and 83 point coordinates were sampled from Degree Confluence Project database (Iwao et al., 2006). We acquired ground truth data by visually interpreting presence of urban at each point coordinates using false colour composites of ASTER/VNIR image based on colour tone and texture.

3.2 Classifying Urban Area from ASTER/VNIR using LLGC

Before applying LLGC, we conducted clustering analysis on the images using ISODATA method in which initial number of clusters was 100 and tolerant convergence was 2%.

We applied LLGC method to the clustered images using MODIS Terra + Aqua Land Cover Type Yearly L3 Global 500 m SIN Grid (MCD12Q1) as initial label of urban area. The result represented spatial structure of urban area, such as sparse greenness in urban area and gradual transition in building density between urban and rural area, in much finer resolution than MCD12Q1 (Column (a) and (b) in Figure 2). However, we found that no urban area was classified in some scenes even though urban area was visually recognizable (Column (b) for Karach and Kiev in Figure 2).

Accuracy assessment on the result of LLGC showed 75% user's accuracy, 41% producer's accuracy, 94% overall accuracy, and 0.50 kappa coefficient (Table 2).

3.3 Estimating Probability of Presence of Urban using Logistic Regression

We assigned confidence value of LLGC, slope, DBU of MOD12 and GRUMP (negative value for inside urban area; positive value for outside urban area) to ground truth data, and estimated logistic model for probability of presence of urban by climatic zone (Table 1). Signs of coefficients were corresponded to our assumption and statistically significant at 95% level, except coefficient of slope for tropical zone and dry zone.

Variable	Tropical	Dry	Temperate	Cold
Intercept	-2.440 (< 0.001)	-2.753 (< 0.001)	-2.364 (< 0.001)	-2.383 (< 0.001)
Real-valued classification with LLGC	6.995 (< 0.001)	9.383 (< 0.001)	5.126 (< 0.001)	5.134 (< 0.001)
Slope	0.007 (0.5393)	-0.036 (0.0979)	-0.042 (< 0.001)	-0.044 (< 0.001)
Distance from boundary of MOD12	-23.960 (< 0.001)	-11.527 (< 0.001)	-17.020 (< 0.001)	-6.430 (< 0.001)
Distance from boundary of GRUMP	-4.722 (0.024)	-6.097 (< 0.001)	-3.623 (< 0.001)	0.742 (< 0.001)

Table 1. Coefficients and p-values of logistic regression by climatic zone. Number in each row indicates coefficient for the variable; number in brackets indicates p-values.

	Climatic zone	User's accuracy	Producer's accuracy	Overall accuracy	Kappa coefficient
LLGC	Global	75%	41%	94%	0.50
	Tropical	83%	27%	95%	0.39
	Dry	NaN	0%	97%	NaN
	Temperate	78%	37%	94%	0.48
	Cold	63%	46%	93%	0.50
MOD12	Global	59%	61%	93%	0.56
	Tropical	67%	52%	96%	0.57
	Dry	29%	23%	96%	0.23
	Temperate	55%	62%	93%	0.54
	Cold	62%	57%	93%	0.56
GRUMP	Global	29%	85%	81%	0.36
	Tropical	31%	88%	87%	0.40
	Dry	10%	65%	82%	0.13
	Temperate	26%	86%	79%	0.32
	Cold	29%	79%	82%	0.35
Estimated urban area with logistic regression	Global	74%	49%	94%	0.56
	Tropical	82%	49%	96%	0.59
	Dry	100%	1%	97%	0.09
	Temperate	76%	46%	94%	0.54
	Cold	67%	46%	94%	0.51

Table 2. Result of accuracy assessments on LLGC, MOD12, GRUMP and estimated urban area with logistic regression globally and by climatic zone. In result of LLGC in dry zone, no pixel at validation point data was classified as urban.

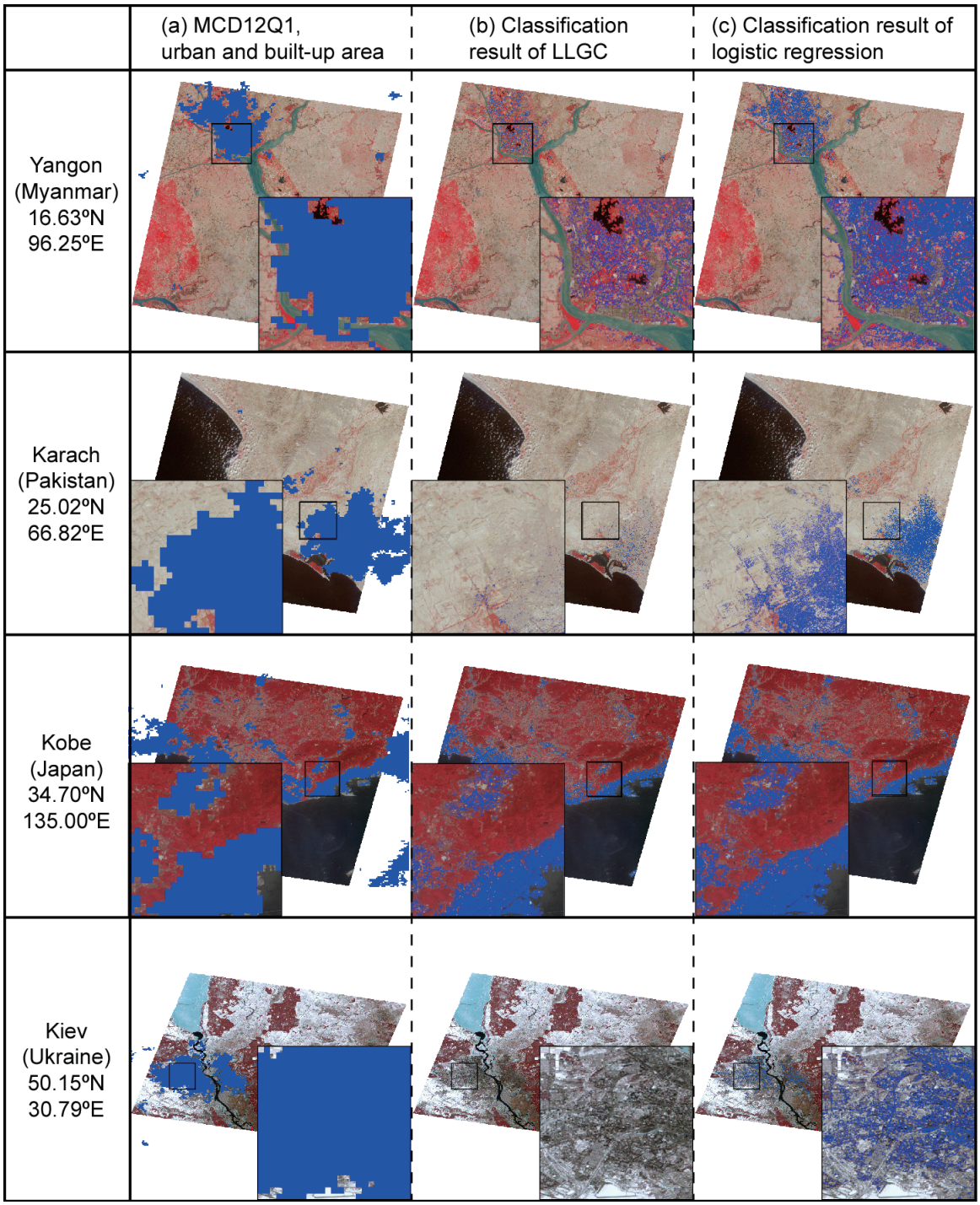

Figure 2: Examples of estimated urban area of MCD12Q1, result of LLGC, and result of logistic regression. Square in image represent extent of close-up image.

We calculated probability of presence of urban for each pixel and classified the pixels into urban or non-urban: Pixels of more than 0.5 probability were classified as urban; pixels of less than or equal to 0.5 probability was classified as non-urban (Column (c) in Figure 2). We assessed accuracy of the classification, showing 74 user's accuracy, 49% producer's accuracy, 94% overall accuracy, and 0.56% kappa coefficient; whereas the accuracies of MOD12 were 59% user's accuracy, 61% producer's accuracy, 91% overall accuracy and 0.56 kappa coefficient; the accuracies of GRUMP were 29% user's accuracy, 85% producer's accuracy, 81% overall accuracy, 0.36 kappa coefficient (Table 2). Higher overall accuracies and kappa coefficients of the results of logistic regression than those of the others indicate improvement in accuracy owing to the integration.

4. DISCUSSION

4.1 Evaluation of LLGC Classification

Higher user's accuracy of LLGC than producer's accuracy of that indicates that LLGC failed to detect much part of actual urban area (Table 2). The main causes of the failures would be so similar surface reflectance among urban and the other non-

vegetated land cover, and thus much urban area was classified as non-urban.

Despite of the misclassifications of LLGC, complex spatial structure of urban area, which was filled with a few pixels in coarse-resolution urban area maps, was very finely represented (Figure 2). Extent of urban area cluster of LLGC was similar to that of MCD12, indicating that LLGC finely trimmed up the clusters of MCD12. It suggests that coarse-resolution urban area map could be improved by LLGC in terms of spatial resolution with keeping original geographical extent of urban area cluster.

4.2 Implication on Coefficients of the Logistic Regression

Difference in degree of the coefficients among climatic zones reflects features of source data. For example, coefficients of DBU of MOD12 for tropical and temperate zone were more significant than that for dry and cold zone. It indicates that, for tropical and temperate zone, estimated urban area in MOD12 was more closely associated to actual urban area than for dry and cold zone. The explanation could be supported by the accuracy assessment, in which kappa coefficients of MOD12 for tropical zone were higher than that for dry and cold zone.

4.3 Improvement with the Integration

The urban area map classified with the integration was more accurate than the result of LLGC, MOD12 and GRUMP in terms of overall accuracy and kappa coefficient (Table 1). Thus we might conclude that the integration improved the accuracy of urban area maps as a whole. Moreover, the integrated map might inherited the features of output of LLGC; that is, user's accuracies of the integrated map (67-100%) were close to that of LLGC (63-83%).

We visually found significant improvements in the result of Karach and Kiev, in which LLGC could not detect some extent of actual urban area, but the integration had done (Column (b) and (c) for Karach and Kiev). The accuracy assessment reflects the improvement, showing higher overall accuracy and kappa coefficient of result of the integration than that of LLGC. If LLGC had failed to detect urban area, the integration would strongly depended on MOD12 and GRUMP; however effect of confidence value of LLGC were remained in the result, shaping complex spatial structure of urban area in 15-m resolution.

5. CONCLUSION

We presented the method for automatic development of urban area map in high resolution using LLGC technique and by integration with existing urban area maps using logistic regression. We implemented the method, and demonstrated it on 340 scenes of ASTER/VNIR as high resolution image, MCD12, MOD12 and GRUMP as existing urban area maps. The result showed LLGC worked effectively to trim up 500m-resolution clusters of urban area into 15m-resolution clusters. The result also showed the integration using logistic regression improved accuracy of urban area maps better than LLGC-derived urban area map and existing urban area maps.

The proposed method will be practically useful for improving accuracy and spatial resolution of global urban area maps. The high-resolution global urban area map developed with the method will encourage providing deeper insights on urbanization not only for developed countries but also for developing countries through regional and international comparisons.

6. ACKNOWLEDGEMENT

This research used ASTER Data beta processed by the AIST GEO Grid from ASTER Data owned by the Ministry of Economy, Trade and Industry of Japan.

7. BIBLIOGRAPHY

Angel, S., S. C. Sheppard, et al., 2005 *The Dynamics of Global Urban Expansion. Transport and Urban Development Department*, The World Bank.

Balk, D., A. Storeygard, et al., 2005 Child hunger in the developing world: An analysis of environmental and social correlates. *Food Policy*, 30(5), pp. 584-611.

Clarke, K., S. Hoppen, et al., 1997 A self-modifying cellular automaton model of historical urbanization in the San Francisco Bay area. *Environ. Plann. Plann. Des.*, 24, pp. 247-262.

Foley, J. A., R. DeFries, et al., 2005 Global Consequences of Land Use. *Science*, 309(5734), pp. 570-574.

Iwao, K., K. Nishida, et al., 2006 Validating land cover maps with Degree Confluence Project information. *Geophys. Res. Lett.*, 33, L23404.

Koeln, G. T., T. B. Jones, et al., 2000 GeoCover LC: Generating Global Land Cover from 7600 Frames of Landsat TM Data. *Proceedings of ASPRS 2000 Annual Conference.*

Laumann, G., 2005 *Science Plan: Urbanization and Global Environmental Change.* Bonn, Germany, International Human Dimensions Programme on Global Environmental Change.

Montgomery, M. R., 2008 The Urban Transformation of the Developing World. *Science*, 319(5864), pp. 761-764.

Nelson, G. C. and R. D. Robertson, 2007 Comparing the GLC2000 and GeoCover LC land cover datasets for use in economic modelling of land use. *Int. J. Remote Sens.*, 28(19), pp. 4243-4262.

Potere, D. and A. Schneider, 2007 A critical look at representations of urban areas in global maps. *GeoJournal*, 69(1), pp. 55-80.

Schneider, A., M. A. Friedl, et al., 2003 Mapping Urban Areas by Fusing Multiple Sources of Coarse Resolution Remotely Sensed Data. *Photogramm. Eng. Rem. S.*, 69(12), pp. 1377–1386.

Scholes, R. J. and R. Biggs, 2005 A biodiversity intactness index. *Nature*, 434(7029), pp. 45-49.

Sutton, P. C., S. J. Anderson, et al., 2009 Paving the planet: impervious surface as proxy measure of the human ecological footprint. *Prog. Phys. Geog.*, 33(4), pp. 510-527.

Yamaguchi, Y., A. B. Kahle, et al., 1998 Overview of Advanced Spaceborne Thermal Emission and Reflection Radiometer (ASTER). *IEEE Trans. Geosci. Remote Sens.*, 36(4), pp. 1062-1071.

Zhou, D., O. Bousquet, et al., 2003 Learning with Local and Global Consistency. *Adv. Neural Inf. Process. Syst.*, 16, pp. 321-328.